In-depth evaluation of a ZrO_2 promoted CaO-based CO_2 sorbent in fluidized bed reactor tests

Andy Antzara[1], Aitor Arregi[1,⊥], Eleni Heracleous[1,2], Angeliki A. Lemonidou[1]*

[1] Department of Chemical Engineering, Aristotle University of Thessaloniki, University Campus, 54124 Thessaloniki, Greece

[2] School of Science & Technology, International Hellenic University (IHU), 14th km Thessaloniki – Moudania, 57001 Thessaloniki, Greece

[⊥] Permanent address: Department of Chemical Engineering, University of the Basque Country UPV/EHU, P.O. Box 644, E48080 Bilbao, Spain

**** Corresponding Authors***

Angeliki A. Lemonidou

e-mail: alemonidou@cheng.auth.gr

phone: +30 2310 996273

fax: +30 2310 996184

Abstract

Carbonate looping, based on the reversible gas-solid reaction of CaO with CO_2, is considered as a promising alternative to amine scrubbing for post-combustion CO_2 capture. Solid sorbents suffer however from degradation, mainly due to thermal sintering and elutriation of fine particles due to enhanced attrition rates in fluidized-bed reactors. In this work, a previously developed synthetic Zr-promoted CaO-based CO_2 sorbent was tested in a fluidized bed reactor unit to determine its performance in cyclic CO_2 capture over various operating conditions, relevant to industrial application. The material exhibited very high carbonation conversion (60-85%) during pre-breakthrough under all investigated conditions, with more than 75% CO_2 removal. The addition of steam in both the carbonation and calcination steps resulted, not only in higher conversions, but also in significantly enhanced cyclic stability. Deactivation was less than 16% after 20 consecutive cycles. The performance of the sorbent was further tested under lower temperature difference between carbonation (680°C) and calcination (750°C), a scheme more favourable for utilizing the heat generated by the highly exothermic carbonation reaction for the thermal demands of the calciner in the actual process. The material displayed similar carbonation conversion, but inferior performance in terms of stability. Advanced post-reaction characterization with in-situ XRD revealed that even though the sintering effect was more limited due to the lower calcination temperature, calcination of $CaCO_3$ was incomplete, rendering a small fraction of the sorbent inactive for CO_2 capture. Under severe calcination conditions (920°C and 80 vol.% CO_2 concentration) the sorbent maintained more than 70% of its initial sorption capacity (7.1 moles of CO_2/kg of sorbent after 20 cycles), a value more than 5 times higher compared to natural limestone.

Keywords: CO_2 capture, Calcium looping, CaO-based sorbents, Zr promotion, Fluidized bed reactor, in-situ XRD

1. Introduction

The increase of atmospheric CO_2 concentration due to anthropogenic activities is the main factor contributing to global warming and the environmental issues that are associated with it [1–3]. The ultimate goal, already adopted by governments in the UN Paris agreement, is the extensive reduction of GHG emissions in order to limit the temperature increase to less than 2°C above 'pre-industrial' levels. This requires essentially a transformation of the industrial power sector that accounts roughly for 2/3 of the anthropogenic GHG emissions [4] and entails the development of new low-carbon technologies and high plant efficiency. It also necessitates the application of new CO_2 capture and storage (CCS) technologies that ensure strong reduction of the net CO_2 emissions, as the current energy sector relies mainly on large stationary installations.

The only large scale CO_2 capture technology currently available is amine scrubbing [5,6]. Although a well-established technology, the installation and operation of these systems comes with a significant penalty on the plant's efficiency [7–10]. Therefore, extensive research efforts are directed towards new improved technologies that can reduce the cost and energy requirements of CO_2 separation, including processes using solid CO_2 sorbents such as zeolites, activated carbons, hydrotalcite-like compounds, alkali zirconates/silicates and calcium oxides [11–15].

Among the potential sorbents for CO_2 capture, probably the most attractive materials are CaO-based solids due to their wide availability, low cost, high theoretical CO_2 sorption capacity and fast carbonation/calcination kinetics [16]. During continuous operation, a CaO-based sorbent undergoes high temperature sorption/desorption cycles (Carbonate Looping) based on the reversible gas-solid carbonation reaction of CaO with CO_2 contained in the flue gases (Eq. 1). CO_2 is absorbed by CaO to form $CaCO_3$ in the capture phase. After saturation of the material, the captured CO_2 is released as a pure,

ready for sequestration stream, according to the reverse process of the reaction which takes place in a second reactor at higher temperatures [17–23].

$$CaO_{(s)} + CO_{2(g)} \leftrightarrow CaCO_{3(s)}, \quad \Delta H_{298K} = -178 kJ/mol \qquad (1)$$

Despite the significant advantages of the reversible carbonation reaction in Carbonate Looping, the process faces two major practical difficulties towards complete commercialization. The first challenge rests in the loss of sorption capacity over successive carbonation/calcination cycles, due to the intense sintering of CaO at the high calcination temperatures employed during the calcination step [24]. In addition to the deactivation problem, the physical strength of the sorbent material is another significant property of concern for CaO-based sorbents. The use of dual fluidized bed reactors is considered the most suitable configuration, in order to have good contact between the solid and gas phases, high heat transfer and reaction rates, as well as continuous operation [25,26]. However, significant attrition and mechanical strength loss have been reported even after only a few carbonation/calcination cycles, especially when natural minerals are used. *Jia et al* [27] tested five different limestones in a pilot scale circulating fluidized bed unit, reporting severe fragmentation and high loss of material, mainly during the initial cycles. Similar results were reported by *Lu et al* [28], with a very high material loss due to attrition (~30% of the initially loaded material) only after 3 cycles.

Various methods have been proposed and applied in order to improve the cyclic performance of the natural sorbents, including thermal or acid treatment [29–32], reactivation through water or steam hydration to improve the surface morphology of the material [33–35] and incorporation of inert chemical additives in the structure of CaO to increase resistance to high temperature sintering [14,36–42]. Different synthesis methods have also been employed with the aim to develop sorbent materials with

improved stability and mechanical strength, including precipitation methods, dry or wet mixing, flame spray pyrolysis and several modified sol-gel routes [14,36,38,43–47]. It should be noted that the preparation route plays an important role in the mechanical strength of the sorbent and therefore on the final performance under fluidized bed conditions. However, up to date, most of the synthesized CaO-based CO_2 sorbents, have been mainly evaluated in TGA apparatuses in powder form, thus rendering the obtained results of little practical relevance.

We have performed extensive work on the synthesis of mixed CaO-based CO_2 sorbents with inert promoters, such as Al_2O_3, ZrO_2, La_2O_3 and MgO via a sol-gel auto-combustion route, in order to stabilize the CaO structure [48]. Preliminary evaluation in TGA showed that the Zr-promoted CO_2 sorbent exhibits excellent performance. The sorbent was extensively tested in cyclic bench scale experiments in a fixed bed reactor in intensified sorption enhanced chemical looping steam methane reforming (SE-CL-SMR) [49] and post combustion CO_2 capture [50]. The material demonstrated more than 80% CaO conversion during the first cycles in both tests and good stability, with less than 5% loss of capacity after 20 cycles in the case of the SE-CL-SMR test, compared to 23% for the carbonation/calcination experiment of CO_2 capture from flue gases. The improved stability of the sorbent during the cyclic SE-CL-SMR experiment could be mainly attributed to the much higher amount of steam used, which has been shown to positive influence the performance of CaO-based sorbents [51].

The main focus of this work was to investigate the performance of the optimized Zr-promoted CaO-based CO_2 sorbent in a fluidized bed reactor for post-combustion CO_2 capture under more realistic conditions. Different crucial operating parameters, such as fluidization velocity, space velocity, presence of steam in the feed stream of the reactor, temperature during carbonation and calcination steps as well as calcination conditions

(high temperature combined with high CO_2 partial pressure), were investigated. The textural properties and the morphology of the sorbent before and after the tests were carefully examined to elucidate the decay trends under the investigated conditions. In addition, we monitored the cycling under carbonation and calcination conditions with in-situ XRD to study in real time structural changes of importance to sorbent degradation.

2. Experimental section

2.1 CO_2 Sorbent synthesis

The CaO-based CO_2 sorbent promoted with ZrO_2 was synthesized using a sol-gel auto-combustion route. The starting materials were calcium nitrate ($Ca(NO_3)_2 \cdot 4H_2O$, ≥99.0%, J.T. Baker) and zirconyl nitrate ($ZrO(NO_3)_2 \cdot xH_2O$, 99.5%, Acros), while citric acid ($HOC(COOH)(CH_2COOH)_2 \cdot H_2O$, ≥99.0%, J.T. Baker) was employed as combustion agent. The sorbent was prepared with a nominal 66 wt.% concentration of free CaO (a Ca/Zr atomic ratio of 7.2 was used for the synthesis of the final material). A stoichiometric molar ratio of nitrate salts/combustion agent was used (9/5), assuming that the gaseous by-products of the combustion reaction between citric acid and nitrate salts were only CO_2, H_2O and N_2 [48]. For the synthesis, the appropriate amount of calcium nitrate and zirconyl nitrate were dissolved in distilled water under continuous heating and stirring. When the temperature of the solution reached 70°C, the combustion agent was added and the temperature was then increased to 120°C under continuous stirring until the occurrence of gelation. The formed gel was transferred to a pre-heated furnace at 300°C, where after a few minutes the gel auto-combusted in a self-propagating combustion manner leading to the formation of a voluminous powder. After calcination at 900°C for 1.5h under air flow (200ml/min), the final powders were

pelletized in small discs in a manual hydraulic press (Specac's Atlas series). The pellets were then crushed and sieved in order to obtain a particle size of $355 < d_p < 500\mu m$.

For the fluidized bed experiments under severe calcination conditions (see section below), a natural limestone provided by *Titan Cement Company* in Greece was also examined as a reference sorbent. The limestone was initially calcined at 900°C for 1.5h under air flow (200ml/min) in order to decompose $CaCO_3$ to CaO. After calcination the material was pelletized, crushed and sieved to the same particle size range with the synthetic sorbent.

2.2 Performance evaluation

2.2.1 Thermogravimetric analysis

The performance of the as received $CaO/CaZrO_3$ powders after calcination and the material after pelletization was evaluated by thermal gravimetric analysis (TGA), in a SDT Q600 instrument for 50 consecutive sorption-desorption cycles, as previously described [48]. About 10mg of material was placed in the sampleholder of the TGA instrument. Prior to the cyclic experiments, the materials were pretreated for 10 minutes at 850°C in nitrogen to remove physisorbed CO_2 and/or H_2O. The CO_2 capacity of the synthesized sorbents was tested under a 15 vol.% CO_2 flow in N_2 for 30 minutes at 650°C. The temperature was then raised to 850°C with a heating rate of 10°C/min and desorption took place under 100% N_2 flow for 5 minutes at 850°C. The chamber was cooled to 650°C with a rate of 50°C/min to 650°C and the cycle was repeated.

2.2.1 Fluidized bed tests

Cyclic carbonation and calcination experiments were conducted at atmospheric pressure in a bench scale laboratory flow unit. The unit consists of the gas feed section, a fluidized bed reactor and the gas analysis section. The incoming gases are controlled by mass flow controllers and pre-mixed before entering the reactor. The fluidized bed quartz reactor (18 mm internal diameter), with coaxial thermocouples for temperature monitoring, was heated electrically by a tubular furnace, with three independently controlled temperature zones. A fritted quartz disk placed in the center of the reactor was used to hold the bed material. Two series of experiments were performed, with carbonation and calcination carried out in the presence or absence of steam. Carbonation was conducted at 650 and 680°C under 10 vol.% CO_2/3.2 vol.% O_2/N_2 feed (*dry conditions*) or 10 vol.% CO_2/20 vol.% H_2O/3.2 vol.% O_2/N_2 feed (*wet conditions*). The percentages of CO_2 and H_2O in the feed were chosen to be representative of typical concentrations in flue gases of a natural gas power plant. Calcination was conducted at higher temperature (750, 800°C) in a pure N_2 flow in the absence of steam, or a 20 vol.% H_2O/N_2 flow in the case of wet conditions experiments. The sorbent was further tested under *harsh calcination conditions*, i.e. calcination in a highly concentrated CO_2 stream (20 vol.% H_2O/CO_2 flow) and at higher temperature (920°C). For comparison reasons a calcined natural limestone was also evaluated under the same relevant conditions. The outlet stream of the reactor was cooled to condensate steam and the CO_2 concentration was then monitored online by a CO_2 analyzer (Horiba, VIA 510). The conversion of CaO in the sorbent (carbonation conversion) was expressed as the number of CO_2 moles captured by the sorbent in a specific timeframe divided by the theoretical maximum capacity of the CO_2 sorbent, according to the following equation:

$$X, \% = \frac{\text{moles of } CO_2 \text{ captured}_{\text{experimental}}}{\text{Max moles of } CO_2 \text{ captured}_{\text{theoretical}}} \quad (2)$$

The percentage of CO_2 captured during carbonation was expressed as the moles of CO_2 captured by the sorbent divided by the moles of CO_2 in the inlet stream of the reactor:

$$CO_2 \text{ capture}, \% = \frac{\text{moles of } CO_{2,in} - \text{moles of } CO_{2,out}}{\text{moles of } CO_{2,in}} \quad (3)$$

Details on material bed, temperatures as well as gas flow conditions (flows, fluidization and space velocities) during carbonation and calcination stages for the different experiments performed are listed in Table 1. According to the specific conditions of each experiment, a material bed length between 3 and 4.5 cm was achieved under cold fluid conditions.

Table 1: Experimental conditions during Carbonate Looping tests

		Carbonation					Calcination				
	Sorbent quantity (g)	**T** (°C)	**Environment** (vol. %)	**GHSV** (h^{-1})	**U/U_{mf}** (-)	**Flow** (ml/min)	**T** (°C)	**Environment** (vol. %)	**GHSV** (h^{-1})	**U/U_{mf}** (-)	**Flow** (ml/min)
66wt% $CaO/CaZrO_3$ synthetic CO_2 sorbent											
Test 1: Effect of fluidization velocity[1]	2.73	650	10%CO_2/3.2%O_2/N_2	3500	3.8	400	800	100% N_2	3100	3.8	355
Test 2: Effect of fluidization/space velocity[1]	1.76	650	10%CO_2/3.2%O_2/N_2	3500	2.5	260	800	100% N_2	3100	2.5	230
Test 3: Effect of space velocity[1]	3.07	650	10%CO_2/3.2%O_2/N_2	2000	2.5	260	800	100% N_2	1700	2.5	225
Test 4: Effect of steam[2]	3.07	650	10%CO_2/20%H_2O/3.2%O_2/N_2	2500	3.1	325	800	20% H_2O/N_2	2150	3.1	280
Test 5: Effect of carbonation/ calcination temperature[2]	2.97	680	10%CO_2/20%H_2O/3.2%O_2/N_2	2500	3.1	315	750	20% H_2O/N_2	2300	3.1	290
Test 6: Effect of calcination conditions[3]	3.07	650	10%CO_2/20%H_2O/3.2%O_2/N_2	2500	3.1	315	920	20% H_2O/CO_2	2000	3.1	260
Natural calcined limestone											
Test 7: Effect of calcination conditions[3]	4.60	650	10%CO_2/20%H_2O/3.2%O_2/N_2	3650	3.1	480	920	20% H_2O/CO_2	2850	3.1	375

[1] Experiments under dry conditions
[2] Experiments under wet conditions
[3] Experiments under severe calcination conditions

2.3 Post-reaction characterization

Different characterization techniques (BET surface area measurements, morphology examination with SEM, structure identification of the material at different stages of the reaction with in-situ XRD) were used in order to provide supplementary information on the performance of the sorbent during the different experimental conditions applied. The fresh and used materials were characterized for all methods in the as received form (crushed and sieved pellets), except for the in-situ XRD tests where very fine powders were required for the measurement.

BET surface area and pore volume were measured by using nitrogen physisorption at 77K with an Autosorb-1 Quantachrome flow apparatus. Prior to the measurements, the samples were degassed in vacuum at 250°C overnight.

In order to identify the reasons for the different stability behavior during fluidized bed experiments, the used materials were characterized with in-situ XRD in a PANalytical Empyrean diffractometer. The measurements were carried out using CuKα1 radiation (α= 1.5406 Å) and a step size of 0.026 degrees. An Anton Paar XRK 900 in-situ high temperature (25-900°C) and high pressure (1-10 bar) reactor cell was used. The experiments were done at atmospheric pressure. Prior to the cyclic experiments, the materials were pretreated for 10 min at the calcination temperature in N_2 to remove any physisorbed CO_2 and/or H_2O. The CO_2 capacity of the synthesized sorbents was tested under a 10 vol.% CO_2/1 vol.% H_2O flow in N_2 for 20 min at sorption temperature. The sample was then heated under pure N_2 flow to the calcination temperature (800°C or 750°C) with a heating rate of 10°C/min and desorption took place under 1 vol.% H_2O in N_2 for 10 min at calcination temperature. After cooling the reactor cell to the carbonation temperature in pure N_2 with a rate of 10°C/min, the cycle was repeated. The

stability of the material was tested for 20 consecutive carbonation/calcination cycles. About 70-100 mg sample powder was used for each experiment.

The carbonation conversion during the in-situ XRD cycles was expressed as the reduction of the area of the main CaO peak (37.2° 2θ) at the end of the carbonation step divided by the maximum CaO area after calcination in each cycle, according to the following equation:

$$X,\% = \frac{\max A_{CaO,2\theta=37.2^\circ} - A_{CaO,2\theta=37.2^\circ,t=20min}}{\max A_{CaO,2\theta=37.2^\circ}} \quad (4)$$

The morphology of the fresh and used sorbents was examined by scanning electron microscopy (SEM) on a JEOL 6300 microscope, coupled with energy-dispersive X-ray analysis (EDX; Oxford Link ISIS-2000) for local elemental composition determination.

3. Results and discussion

3.1 Preliminary evaluation in TGA

Prior to the fluidized bed experiments, the sorbent was tested both in powder and pellet form in a TGA instrument in order to check the effect of pelletization in the performance of the material to be used in the bench scale unit. Carbonation conversion and sorption capacity of $CaO/CaZrO_3$ powders and pellets in the TGA instrument is presented in Figure 1. It can be observed that the material showed a similar initial high sorption capacity of ~10.9 moles of CO_2/kg of sorbent even after pelletization, which corresponds to 93% CaO conversion. In terms of stability, the material exhibited very stable performance in both forms, with the pellets showing a slightly higher deactivation rate during the last 10 cycles. This can be probably attributed to loss of interparticle porosity during pelletization. Overall, the pellets showed less than 7% deactivation after

50 consecutive carbonation/calcination cycles, demonstrating the potential of $CaO/CaZrO_3$ composites for CO_2 sorption.

It is generally desirable for CO_2 sorbents to have high sorption capacity, in order to maintain a low amount of material circulating between the two reactors and reduce the overall operating cost. Thus the amount of inert material used as structural stabilizer should be minimized. Compared to synthetic materials with lower fractions of inert promoters (9-26 wt.%) reported in literature [43,52–54], or even naturally derived limestones with 100% CaO [34,55–57], the sorption capacity of the herein reported $CaO/CaZrO_3$ sorbent was similar or even higher (6.3-10.2 moles of CO_2/kg). This, in combination with the enhanced sintering resistance of the material, implies reduced operating expenses due to relatively low amounts of sorbent required and low make-up rates, compensating for the higher sorbent cost.

3.2 Fluidized bed experiments

The performance of the $CaO/CaZrO_3$ CO_2 sorbent under different operating conditions was investigated under fluid bed conditions. Various operating parameters such as fluidization and space velocities, steam addition and carbonation and calcination temperatures were studied in order to provide insight on the effect of these conditions on the uptake CO_2 sorption capacity with cycles and the attrition resistance of the material.

3.2.1 Effect of fluidization velocity

Figure 2a illustrates the effect of fluidization velocity on CaO conversion and sorption capacity during the pre-breakthrough region, i.e. where the carbonation of the material

is controlled by the desirable fast surface reaction, for 15 consecutive cycles. Minimum fluidization velocity U_{mf} was calculated by combining Ergun equation [58] with two empirical relationships between sphericity of the particles, φ and void fraction at minimum fluidization, ε_{mf} provided by Wen and Yu [59], resulting on the following generalized correlation [60]:

$$\frac{\bar{d}_p U_{mf} \rho_g}{\mu} = \left[(33.7)^2 + 0.0408 \frac{\bar{d}_p^3 \rho_g (\rho_s - \rho_g) g}{\mu^2} \right]^{1/2} - 33.7 \quad (5)$$

where $\bar{d}_p$ is the mean particle diameter, ρ_g and ρ_s are the gas and solid density respectively and μ the gas viscosity.

The flow rates during carbonation and calcination steps were adjusted in order to achieve a U/U_{mf} ratio of 2.5 and 3.8, while the amount of material used in each experiment was also altered accordingly in order to maintain a constant space velocity of 3500 h^{-1}. Although the use of lower U/U_{mf} ratios was attempted, homogeneous fluidization could not be attained due to gas flow channeling through the sorbent bed.

As shown in Figure 2a, around 77 % and 70 % CaO conversion was achieved in the 1st cycle with U/U_{mf} ratio of 3.8 and 2.5 respectively, corresponding to a sorption capacity of 9.1 and 8.2 moles of CO_2/kg of sorbent. This sorption capacity was lower than the initial capacity obtained in the TGA experiment (10.9 moles of CO_2/kg of sorbent), which however corresponds to both the pre-breakthrough and breakthrough periods. In terms of stability, the sorbent demonstrated higher deactivation at high fluidization velocity (U/U_{mf}=3.8). A deactivation of 66% was observed after 15 carbonation/calcination cycles, compared to 47% at U/U_{mf} ratio of 2.5. Moreover, the capacity of the sorbent tended to stabilize faster at lower fluidization velocity, with a significant drop in the deactivation rate observed after the first 4 cycles followed by a

more stable performance. At high fluidization velocity (U/U_{mf}=3.8), the same trend was observed only after the 11th cycle.

In an effort to reactivate the sorbent after the first 15 cycles, cycle 16 was extended to achieve complete saturation. It has been argued that in extended carbonation steps, the particle undergoes slow carbonation in the diffusion-controlled regime, something that changes the pore size distribution and ultimately leads to higher reactivity after subsequent calcination [61,62]. As can be seen in Figure 2b, the addition of the prolonged cycle indeed led to the recovery of a large part of the sorbent's initial capacity. However, the decay in conversion continued with comparable rate in the subsequent cycles, leading to a final capacity similar to the one before reactivation of the sorbent after ~25 cycles in total for both fluidization velocities studied. Reactivation of the sorbent had a slight positive effect at high fluidization velocity (U/U_{mf}=3.8), with CaO conversion tended to stabilize faster compared to the initial cycles, leading to a similar final conversion for both fluidization velocities applied.

The carbonation profiles of cycles 1 and 16, in terms of percentage of CO_2 captured during carbonation stage, are presented in Figure 3 for the two fluidization velocities studied. In these two cycles, the carbonation duration was extended to achieve complete saturation of the sorbent, as opposed to all other cycles where the operating mode was switched to calcination at the onset of the breakthrough period (transition from pre-breakthrough to breakthrough was considered to take place when CO_2 concentration in the reactor's outlet stream increases above 2.5%). The profiles indicate that in the first stage (pre-breakthrough period), the rate determining step is the fast surface reaction between CO_2 and CaO. During this period, the CO_2 capture rate was maintained at very high levels, resulting in the removal of over 82% of CO_2 from the flue gases at both fluidization velocities. This is close to the thermodynamically dictated value of CO_2

removal from the flue gases stream at 650°C (~90%, dashed line) [63], indicating that even at the short residence time used in order to achieve high fluidization (GHSV=3500 h^{-1}), the material can capture almost the maximum amount of CO_2. After the formation of the external layer of $CaCO_3$, carbonation of the unreacted CaO was limited by the slower diffusion of CO_2 through this layer, leading to a gradual decrease of the percentage of CO_2 removed from the flue gases. The duration of the pre-breakthrough period during the first cycle was approximately 15.5 min and 14 min when U/U_{mf} ratios of 3.8 and 2.5 were used respectively (Figure 3a). The relatively higher duration when U/U_{mf} ratio of 3.8 was used can be explained by the higher initial conversion achieved with this fluidization velocity. After 16 consecutive carbonation/calcination cycles however, the pre-breakthrough period was reduced to approximately 6 min and 7.5 min for U/U_{mf} ratios of 3.8 and 2.5 respectively with a concurrent increase of the step governed by diffusion of CO_2 through the $CaCO_3$ layer (breakthrough period) for both fluidization velocities used. Even though CO_2 capture during pre-breakthrough remained almost unchanged (Figure 3b), the reduction of the pre-breakthrough duration signifies a severe loss of sorption capacity, especially considering that in a commercial carbonate looping unit the carbonation step would be terminated before the breakthrough point of the sorbent.

3.2.2 Effect of space velocity

The effect of space velocity was investigated at two different GHSVs and constant U/U_{mf} ratio of 2.5. Figure 4 presents the CaO conversion and sorption capacity, as well as the percentage of captured CO_2, during the pre-breakthrough period at space velocities of 2000 and 3500 h^{-1} for 20 consecutive carbonation/calcination cycles. In the 1st cycle, a CaO conversion of around 70-73% was achieved for both space velocities.

After an initial, fast decay of capacity, the carbonation conversion stabilized at around 45% and 37% for space velocities of 2000 h^{-1} and 3500 h^{-1} respectively. The percentage of CO_2 in the flue gases that was captured during the pre-breakthrough period remained at very high levels (81-86%) in every cycle for both experiments (Fig. 4b), with slightly higher values recorded in the experiment with the low space velocity. Even at a high space velocity of 3500 h^{-1} however, the rate of CO_2 capture was high enough to efficiently remove more than 80% of the CO_2 from the flue gases stream at the exit of the reactor. The constant high capture efficiency reveals that the rate of CO_2 capture remains unaffected by deactivation, which simply reduces the available sites of free CaO due to sintering.

3.2.3 Effect of steam

Steam, which is present in the flue gases of a power plant in different concentrations according to the fuel used, has been reported to enhance the performance of CaO-based sorbents [64–67]. Moreover, steam can be also used during calcination as an inert sweep gas, which enables regeneration of the sorbent at relatively lower temperatures. In addition, steam can be easily separated from the desorbed CO_2 by condensation downstream the calciner, delivering a ready-for-sequestration pure CO_2 stream. In order to investigate the effect of steam, a cyclic test was carried out with 10 vol.% CO_2/20 vol.% H_2O/3.2 vol.% O_2/N_2 and 20 vol.% H_2O/N_2 feeds for carbonation and calcination respectively. A constant steam concentration of 20 vol.% was selected as typical of natural gas-fired power plant flue gases with approximately 10% excess air [68]. The other conditions remained almost constant, with only a slight increase of fluidization and space velocities due to steam addition (U/U_{mf} =3.1, GHSV=2500 h^{-1}).

Figure 5 presents the carbonation conversion and the sorption capacity of the sorbent during pre-breakthrough in the presence of steam. Results without steam at slightly different conditions (lower fluidization and space velocity) are also included in the same graph for comparison. Steam addition resulted not only in higher initial conversion during the pre-breakthrough period but also in enhanced stability, with the material exhibiting less than 16% deactivation after 20 carbonation/calcination cycles compared to almost 38% for the experiment performed in the absence of steam. The higher carbonation conversion can be attributed to the enhanced solid-state diffusion of the flue gases through the formed $CaCO_3$ layer in the presence of steam, resulting in a prolonged pre-breakthrough regime [67,69]. The higher conversion during carbonation in addition to the enhanced rates of calcination under wet conditions [64], results in better reconstruction of the porous structure of the material due to larger amount of CO_2 released during calcination step and thus improved cyclic stability.

The above results are better interpreted when comparing the pore size distribution of the sorbent before and after the experiments under dry and wet conditions. As shown in Figure 6, the majority of the pore volume in the used material after dry carbonation is associated with smaller pores (average pore diameter of ~30 nm) compared to the fresh material (28-54 nm). On the contrary, the pores become further enlarged under wet conditions, with average pore diameter slightly above 50 nm. The larger pores are less prone to pore blockage and thus lead to higher conversions. This is also in a good agreement with the critical layer thickness of $CaCO_3$, as determined by *Alvarez and Abanades* [70], beyond which the transition from the fast kinetically controlled reaction to the slow diffusion stage occurs (~50nm). As reported by *Donat et al* [66], there is a synergistic effect when steam is present in both stages, which can be explained by the

enhanced diffusion of CO_2 during carbonation and the larger pores formed during calcination in the presence of steam.

In the presence of steam, the material exhibited better performance both in terms of stability and sorption capacity even compared to fixed bed reactor configuration, presented in our previous work (9.0 moles of CO_2/ kg of sorbent initial capacity and 23% deactivation after 20 consecutive cycles) [50]. Even though almost 8 times higher space velocity was used compared to the fixed bed reactor test in order for the fluidized bed to operate in the bubbling regime, the sorbent demonstrated an excellent performance with an improved initial sorption capacity of 9.9 moles of CO_2/ kg of sorbent and superior stability.

Carbonation profiles for the 1st cycle and 20th cycle with and without steam are shown in Figure 7a and 7b respectively. The length of these cycles was extended to achieve complete saturation. Similar duration of pre-breakthrough period (21-23 min) was recorded in both experiments for the first cycle (Figure 7a). Even though in the experiment with steam a higher CO_2 flow was used in order to maintain a constant CO_2 concentration of 10% in the reactor's inlet stream, the sorbent reached the breakthrough point at approximately the same time with the test without steam due to higher sorption capacity during the kinetically controlled regime. Moreover, the breakthrough period was very short with the use of steam, with the sorbent saturating rapidly after reaching a carbonation conversion of 84% at the breakthrough point. In the absence of steam, the carbonation reaction fell into diffusion-controlled regime much earlier, after only ~73% carbonation of the material. In both experiments the sorbent reached an overall CaO conversion over 95% after the post-breakthrough period (Table 2), indicating that steam addition basically results in faster capture of the CO_2. Similar findings from fluidized bed tests with steam addition have been also reported in studies of other groups, with a

remarkable increase of sorption capacity both for natural [71] and synthetic sorbents [55] being observed.

After 20 carbonation/calcination cycles the duration of the kinetically controlled regime decreased in both cases, with the phenomenon being more pronounced in the absence of steam. On the other hand, the diffusion controlled period increased, indicating modification of the morphology of the material with cycling. In the presence of steam the sorbent was completely saturated in CO_2 after ~60 min, while more than 120 min were required in dry conditions. As also shown in Table 2, the overall carbonation conversion of the sorbent after 20 cycles remained stable in both experiments despite the slower diffusion, indicating that the intrinsic capacity of the materials did not change.

Table 2: Conversions and durations of pre-breakthrough period and overall carbonation stage during 1st and 20th under dry and wet conditions.

	Cycle 1				**Cycle 20**			
	CaO conversion (%)		**Duration (min)**		**CaO conversion (%)**		**Duration (min)**	
	Pre-BT[a]	Overall	Pre-BT[a]	Overall	Pre-BT[a]	Overall	Pre-BT[a]	Overall
Without steam	73.4	97.2	23	40	45.4	96.2	14	125
20% steam	84.1	95.7	21	30	70.9	97.8	18	65

[a]Pre-breakthrough period

3.2.4 Effect of carbonation/calcination temperatures

To reduce the overall thermal requirements of the Carbonate Looping process, it is desirable to operate the carbonator and the calcinator at similar temperatures to enable efficient heat integration. In this context, an experiment was performed with carbonation and calcination carried out at 680°C and 750°C respectively in the presence of steam. The results obtained from experiments with different temperatures protocols are compared in Figure 8. Even though similar sorption capacity was recorded in both cases during the first cycle, the use of lower ΔT between carbonation and calcination led to faster deactivation of the sorbent (28% vs 16% after 20 cycles).

CO_2 capture profiles during the carbonation step of the 1st cycle and 20th cycle are presented in Figure 9a & 9b for the two different carbonation temperatures (650°C and 680°C respectively). As expected, lower CO_2 removal was recorded at 680ºC, due to equilibrium limitations of the strongly exothermic carbonation reaction. Nevertheless, even at 680°C around 75% of the CO_2 was captured during pre-breakthrough in almost every cycle, albeit with longer duration. However, after 20 cycles, the duration of the pre-breakthrough period decreased by approximately 8 min (from 26 to ~18 min) at 680°C (Figure 9b), compared to only 3 min (from 21 to 18 min) for the experiment where carbonation is carried out at 650°C (Figure 9a), indicating that deactivation was faster when a narrower ΔT between carbonation and calcination steps is applied. In addition to the reduction of the pre-breakthrough period, a slight decrease of the CO_2 captured was observed for both experiments. This result is contrary to expectations, as higher cyclic deactivation is expected to occur at higher calcination temperatures due to more intense thermal sintering [56,72]. In order to shed light on the origins of the observed performance, advanced characterization with in-situ XRD was performed, as discussed in detail in the post-reaction characterization section (§ 3.3).

3.2.5 Evaluation under severe calcination conditions

In the industrial application of the Carbonate Looping process, it is very important to perform calcination under CO_2 atmosphere in order to produce a concentrated, ready for sequestration CO_2 stream. However, the higher temperature required to enable adequate calcination rates (>900°C) under high CO_2 partial pressures, combined with the CO_2 atmosphere, can lead to increased deactivation due to enhanced sintering [72,73]. Therefore, an additional test was performed, where calcination was carried out at higher temperature (920°C) and a stream with high CO_2 concentration (80 vol.%). For comparison reasons a calcined natural limestone was also evaluated under the same conditions.

Figure 10 presents the sorption capacity during pre-breakthrough of natural limestone and $CaO/CaZrO_3$ sorbent. A similar initial sorption capacity was recorded both for the synthetic sorbent and the natural limestone (10.1-10.3 moles of CO_2/kg). Considering that the $CaO/CaZrO_3$ sorbent has lower CaO loading (66 wt.%), the synthetic sorbent exhibits much higher conversion during pre-breakthrough compared to limestone, also similar to the mild operating conditions (calcination at 800°C in H_2O/N_2 flow, see Figure 8 for details). This can be mainly attributed to the much higher surface area of the synthetic sorbent (20.9 m^2/g) compared to calcined limestone (8.3 m^2/g). The most notable difference between the two materials is their cyclic stability. The natural limestone demonstrated fast deactivation during the first 3-4 cycles with this deterioration tending to decrease in the subsequent cycles, resulting in a residual capacity of ~1.3 moles of CO_2/kg (~7% carbonation conversion). This is in good agreement with the results reported by *Grasa and Abanades* [56], who tested different limestone samples in long series of carbonation/calcination cycles in TGA with calcination temperatures up to 950°C. They reported a dramatic decrease of conversion

during the first cycles, which stabilized around a residual conversion of 0.075-0.08% after 50 or more cycles. The $CaO/CaZrO_3$ synthetic material exhibited a very stable performance even under these harsh conditions, maintaining more than 70% of its initial sorption capacity after 20 carbonation/calcination cycles. This final capacity is almost 5.6 times higher compared to limestone, demonstrating the excellent performance of the synthesized material also under severe conditions.

CO_2 capture versus time during carbonation in the 1st cycle and 20th cycle are presented in Figures 11a & 11b for the natural limestone and the $CaO/CaZrO_3$ sorbent respectively. A similar pre-breakthrough duration of ~22 min was recorded during the first cycle for both materials, even though a higher CaO/CO_2 molar ratio was used for the calcined limestone due to the higher free CaO concentration (100wt. vs 66wt. % for the synthetic material). As shown in Figure 11a, after the breakthrough point the CO_2 capture reached a minimum value of <10% very fast, indicating that CO_2 diffusion through $CaCO_3$ is very limited, due to blockage of the pores. This is also evidenced by the similar pre-breakthrough and overall carbonation conversions in the first cycle, as shown in Table 3. Regarding the synthetic sorbent, in addition to the higher conversion during pre-breakthrough, the material continued to absorb CO_2 with a relatively high rate even during the diffusion-controlled stage, resulting in an overall conversion of 97.1% after 45 min. After 20 carbonation-calcination cycles, the duration of pre-breakthrough period decreased for both materials, with the reduction being more severe for the limestone. Moreover, for both materials, CaO was not completely saturated after breakthrough, with carbonation proceeding with a very slow rate. As a result, after 85 and 55 min, overall conversions of 22.4% and 91.4% were recorded for limestone and $CaO/CaZrO_3$ respectively (Table 3). This is a significant difference compared to the results obtained under mild calcination conditions (Table 2), where the intrinsic sorption

capacity of the $CaO/CaZrO_3$ was maintained even at prolonged carbonation periods. This indicates that under realistic conditions, sintering of the materials is more severe and a small part of the porous structure of CaO is irreversibly destroyed.

An additional important point that cannot be ignored in practical applications of post-combustion CO_2 capture is related to the additional decrease of CO_2 sorption capacity due to the presence of SO_2 in the flue gases [74–76]. CaO can also react with SO_2 to form $CaSO_4$, however irreversibly under typical Carbonate Looping conditions, rendering a fraction of the sorbent inactive in CO_2 capture. Therefore, unless a high make-up flow is used for the sorbent, SO_2 removal prior to CO_2 capture is probably essential in order to achieve a reduced operating cost, especially for synthetic materials. As a next step in our study, we plan to evaluate the material under industrially relevant conditions with SO_2 present in the simulated flue gases, in order to check the tolerance of $CaO/CaZrO_3$ in the sulfation reaction.

Table 3: Conversions and durations of pre-breakthrough period and overall carbonation stage during 1st and 20th under severe calcination conditions for the natural limestone and the synthetic $CaO/CaZrO_3$ CO_2 sorbent

	Cycle 1				**Cycle 20**			
	CaO conversion (%)		**Duration (min)**		**CaO conversion (%)**		**Duration (min)**	
	Pre-BT[a]	Overall	Pre-BT[a]	Overall	Pre-BT[a]	Overall	Pre-BT[a]	Overall
Natural limestone	57.7	66.3	21	50	7.1	22.4	2.5	85
$CaO/CaZrO_3$	85.0	97.1	22	50	60.1	91.4	15.5	55

[a]Pre-breakthrough period

3.3 Post reaction characterization

BET surface areas and pore volumes of fresh and used sorbents are presented in Table 4. The surface area of the spent $CaO/CaZrO_3$ sorbent after 19 carbonation/calcination cycles in the absence of steam decreased from ~21 m^2/g to 13.2 m^2/g, with the pore volume following a similar trend. When steam was present, the spent sorbent maintained a large part of its initial surface area, while the pore volume slightly increased. As previously suggested, the presence of steam significantly reduces diffusion resistance of the flue gases through the $CaCO_3$ product layer to less easily accessible CaO sites, resulting in a delay of the transition from the kinetically to the diffusion controlled regime, leading to higher conversion. Due to the higher conversion, the CO_2 evolved in the calcination step is higher, resulting in better reconstruction of the porous structure of the material and leading to improved stability with cycles [77]. This is consistent with the more stable performance of the sorbent in the presence of steam. When calcination was performed at 750°C instead of 800°C, the surface area loss was more limited (18.3 m^2/g), due to the as expected lower sintering.

Table 4: BET surface area and pore volume of fresh and used $CaO/CaZrO_3$ sorbents after different experimental protocols.

	Surface area (m^2/g)	**Pore volume (cm^3/g)**
$CaO/CaZrO_3$_fresh	20.9	0.12
$CaO/CaZrO_3$_spent_650°C/800°C_Without steam	13.2	0.10
$CaO/CaZrO_3$_spent_650°C/800°C_20% steam	15.2	0.13
$CaO/CaZrO_3$_spent_680°C/750°C_20% steam	18.3	0.14

The above results are also supported by the SEM micrographs of the sorbent, obtained before and after each experiment (Figure 12). The images of the fresh sample (Figure 12a & 12b) and after 19 carbonation/calcination cycles in the absence of steam (Figure 12c & 12d) show the changes in the morphology of the material. The spent sorbent is characterized by a more compact surface morphology with loss of porous areas and larger grains, as a result of sintering of the formed $CaCO_3$ at the high calcination temperatures.

With steam addition, the spent sorbent seems to maintain a granular morphology similar to the fresh material for both temperature protocols employed (Figure 12e-h). In the case of calcination at 750°C, even smaller grains are apparent, compared to the fresh sorbent. It can thus be suggested that in the presence of steam the morphology of the material was rather reconstructed than preserved, resulting in generation of additional pores during calcination in each cycle, consistent with the slight increase of the pore volume of the spent sorbents (Table 4).

In-situ XRD was employed to investigate in-depth the structural changes that occur when different temperature protocols are applied. For this, fresh and used sorbents obtained after the carbonation step of the 19^{th} cycle from the experiments carried out using different temperatures during carbonation (650/680°C) and calcination (800/750°C) were used. For brevity, the two experimental protocols are herein denoted as H-ΔT and L-ΔT, for the high (650/800°C) and the low (680/750°C) temperature difference between carbonation and calcination.

The two used sorbents after pre-breakthrough of the 19^{th} cycle were initially scanned in-situ in the reactor cell at room temperature. As shown in Figure 13, both CaO and $CaCO_3$ were detected in both used samples, with however different intensity. The $CaCO_3$/CaO ratio is much higher in the sorbent after the H-ΔT (Figure 13a) compared to

the L-ΔT test (Figure 13b), consistent with the higher measured carbonation conversion. The calcined samples after the 19th cycle under H-ΔT and L-ΔT fluidized bed tests were re-exposed to calcination in 1vol.% H_2O/N_2 in the reactor cell of the in-situ XRD instrument under the respective temperature conditions. In both scans taken at high temperatures there is a shift in the diffraction peaks positions towards lower 2θ values compared to the room temperature scans, due to thermal expansion of the lattice [78]. For the H-ΔT spent sample, calcination at 800°C led to complete decomposition of $CaCO_3$ to CaO (Figure 13a, diffractrogram 2). On the contrary, in the case of the L-ΔT sample, peaks characteristic of $CaCO_3$ are still present after calcination at 750°C, indicating that a small part of the material may still be in carbonated form even after the calcination step of the continuous cycles (Figure 13b, diffractrogram 2). This could explain the lower performance of the sorbent in terms of stability during the fluidized bed experiment, since an accumulating fraction of CaO became inactive as it exited the calcination step in carbonated form already. As mentioned above, the effect of sintering was less pronounced when the L-ΔT protocol was applied, resulting in limited surface area reduction (Table 4). This however also implies that the fraction of $CaCO_3$ in the calcined material at 750°C is not very high, since a high proportion of carbonated sorbent would lead to extensive surface area loss. In order to confirm this point, the fraction of $CaCO_3$ in the sorbent after calcination at 750°C was calculated from the CaO and $CaCO_3$ peak as explained in the experimental section and was found to be less than 8 wt.% of the sorbent (including the inert mixed phase).

Figure 14 shows the carbonation conversion of the fresh and used sorbents from the H-ΔT (Fig. 14a) and L-ΔT (Fig. 14b) tests during 20 carbonation/calcination cycles in in-situ XRD. The conversion was calculated by quantifying the area of the main CaO peak (37.2° 2θ). The conversion of CaO during the bench-scale tests is also presented in the

same graphs for comparison. A good agreement is observed between the results obtained in the fluidized bed reactor test and the reactor cell of the XRD instrument at both carbonation temperatures, despite the differences in the flow patterns. Even with much lower steam concentration (1 vol.%) during the carbonation/calcination cycles in the in-situ XRD setup compared to the fluidized bed reactor (20 vol.%), it was possible to achieve similar high conversion and stability. This indicates that even small amounts of steam suffice to observe its positive influence, in good agreement with previously report results [66,67]. As argued by *Donat et al* [66], the effect of steam on the sorption capacity, for low steam concentrations is mainly reliant on the available amount of steam with no further improvement above some saturation point, which can be as low as 1-3 vol.% depending on the sorbent material.

With regards to the used sorbents from the H-ΔT and L-ΔT tests in the bench scale unit, they exhibit, as expected, lower initial conversion than the fresh material with however higher stability. This confirms that the sorbent tends to further stabilize after an initial loss of capacity, as also observed in the fluidized bed experiments after the first 8-9 cycles.

One of the most important challenges for commercial application of the Carbonate Looping process in fluidized bed configuration is the poor attrition resistance of CaO-based materials. This induces sorbent mass losses and increases the overall cost of the CO_2 capture technology as it necessitates large makeup streams. Attrition resistance is therefore a key property for CO_2 capture solid sorbents. The used $CaO/CaZrO_3$ sorbents after experiments under dry and wet conditions (L-ΔT and H-ΔT protocols) were sieved in order to have a preliminary estimation of the particle size distribution of the material after multiple cycles. The tendency of natural CaO to generate additional fine particles due to its progressive swelling and particle breakage during the gradual hydration to

$Ca(OH)_2$ is a well-known phenomenon [79–82]. As the material was stored in a capped container under ambient conditions, the interaction of CaO with atmospheric moisture cannot be ruled out. To avoid the interference of such phenomena in the interpretation of the results, the fresh material was sieved again before each experiment to obtain the desired particle range (355-500μm). During this additional sieving the percentage of the material lost as fine particles was very low (<5 wt.%), indicating that any collapse of the particle shape due to swelling phenomena was limited.

As shown in Figure 15a, the used material after 20 dry carbonation/calcination cycles exhibited slight agglomeration, with ~1wt% of the particles having size larger than the initial size range (355-500μm). The most striking difference compared to the fresh sample was the formation of smaller particles, with ~18wt. % of the used sorbent being mostly in the range 250-355μm. In the presence of steam, although agglomeration was not observed, attrition of the material was more pronounced. In the used sorbent, about 40wt. % of the particles were equally distributed between the 180-250μm and 250-355μm size ranges. The presence of steam reduces therefore the mechanical strength of the solid, leading to higher attrition rates. As described by *Scala e*t al [83,84], the attrition of sorbent particles can be classified in two main mechanisms. Primary fragmentation of the particles can occur due to thermal stresses, as well as due to excessive internal over-pressures associated with carbonation or calcination reactions, resulting in generation of more coarse-grained fragments. Sorbent particles are also exposed to surface abrasion due to collision with the reactor as well as other particles in the bed, causing a secondary fragmentation which generates easily elutriated fines. Therefore, based on the first attrition mechanism, the higher carbonation and calcination rates in the presence of steam can result in an increased internal pressure and thus increased fragmentation.

Similarly, the $CaO/CaZrO_3$ sorbent and the natural limestone after 20 carbonation/calcination cycles under severe conditions were sieved again and results of particle size distribution are presented in Figure 15b. A slight agglomeration was observed for both materials due to the much higher calcination temperatures (920°C) and the CO_2 atmosphere, with the effect being more pronounced for the natural limestone. The most important difference however is the formation of smaller particles. More than 50 wt.% of the $CaO/CaZrO_3$ sorbent remained in the initial size range, with the formation of smaller particles being limited mostly in the 250-355μm range. On the contrary, fragmentation was more intense for the natural limestone, resulting in the generation of particles in the 100-180μm and 180-250μm size ranges (~7 and 18 wt.% respectively), while almost 20 wt.% of the initial amount elutriated from the material bed in the form of fine particles. Elutriation of the particles occurred mainly during the first 2-3 cycles resulting, in combination with the intense sintering, in an initial high decrease of the sorption capacity as previously shown (Figure 10).

It is important to note that the amount of the synthetic $CaO/CaZrO_3$ material that escaped in the cyclone in the fluidized bed bench scale tests was in all cases negligible. Taking into account however that almost 40 wt.% of the particles after 20 cycles were in a quite smaller size range (180-355μm), it was considered essential to estimate the maximum size of the particles that could likely elutriate from the material bed under the studied conditions. The maximum size of the particles to be spouted from the bed was calculated using the method described by Kunii and Levenspiel [85], assuming that the particles have a terminal free-fall velocity (u_t) equal to the fluidization velocity used in the current experiments in the presence of steam (17.6 cm/s). Using a correlation between U_{mf} and sphericity (Eq. 6) obtained from Pata and Hartman [86], a sphericity (φ_s) of 0.68 was estimated from the minimum fluidization velocity. Based on the

equations below (7-9), a dimensionless particle size d_p^* and a dimensionless terminal velocity U_t^* can be introduced, which allow the direct evaluation of particle size d_p for a given terminal velocity U_t. The maximum expected size of particles elutriating at these conditions is around 110 μm, which is much smaller than the smallest size range of particles formed during the cyclic experiments. This indicates that it is possible to operate under fluidized bed conditions in the bubbling regime without significant attrition and material loss.

$$U_{mf} = \frac{(\varphi_s d_p)^2}{150} \frac{\rho_s - \rho_g}{\mu} g \frac{\varepsilon_{mf}^3}{1-\varepsilon_{mf}} \quad (6)$$

$$d_p^* = d_p \left[\frac{\rho_g(\rho_s - \rho_g)g}{\mu^2} \right]^{1/3} \quad (7)$$

$$U_t^* = U_t \left[\frac{\rho_g^2}{\mu(\rho_s - \rho_g)g} \right]^{1/3} \quad (8)$$

$$U_t^* = \left[\frac{18}{(d_p^*)^2} + \frac{2.335 - 1.744\varphi_s}{(d_p^*)^{0.5}} \right]^{-1}, \qquad 0.5 < \varphi_s < 1 \quad (9)$$

4. Conclusions

In this work, we evaluated a previously developed synthetic $CaO/CaZrO_3$ CO_2 sorbent prepared by sol-gel auto-combustion in a bench-scale fluidized bed reactor unit under different operating conditions (fluidization velocity, space velocity, steam during carbonation and calcination and temperatures of carbonation and calcination steps, CO_2 partial pressure during calcination). The sorbent demonstrated superior performance, with high carbonation conversion recorded during pre-breakthrough region (60-85%) under all investigated conditions. Even at the high space velocities required for

fluidization, the material maintained a fast carbonation rate, leading to a CO_2 capture from the flue gases of over 80% and 75% at carbonation temperatures of 650 and 680°C respectively. The addition of steam led to higher conversions, especially during pre-breakthrough, due to decreased diffusion resistance of CO_2 through the formed layer of $CaCO_3$. In addition, steam significantly enhanced the stability of the sorbent, leading to <16% deactivation after 20 consecutive cycles. When the sorbent was tested in tests with smaller temperature difference between carbonation (680°C) and calcination (750°C), it exhibited similar carbonation conversion but higher deactivation. Advanced characterization with in-situ XRD showed that even though the sorbent largely retains its initial high surface area and porous morphology, $CaCO_3$ decomposition is incomplete at 750°C, rendering a small fraction of the sorbent inactive for CO_2 capture. The sorbent also exhibited satisfactory mechanical strength. Even though almost 40% of the material shattered into smaller fragments in the presence of steam, attrition was limited to generation of particles in the range of 180-355μm, with no mass loss due to fines elutriating from the bed. Finally, the material demonstrated an excellent performance even under severe calcination conditions (i.e. calcination in high CO_2 partial pressure and higher temperature), maintaining more than 70% of its initial sorption capacity after 20 cycles. Compared to a natural limestone that was used as reference material, the final capacity of $CaO/CaZrO_3$ was almost 5.6 times higher. Although the cost of a synthetic material, such as the one reported in this work, would apparently be higher than that of a natural sorbent, the increased sorption capacity and stability, even under severe calcination conditions, are expected to lead to much lower amount of material circulating between the two reactors and a minimum required sorbent make-up flow, balancing the increased synthesis cost.

Acknowledgments

We acknowledge the financial support from European Union-European Regional Development Fund and Ministry of Development, ESPA 2007–2013/EPAN II programme, Action Synergasia11'.

Financial support by the Access to Research Infrastructures activity in the Horizon 2020 Programme of the EU (ECCSEL INFRADEV-3 Grant Agreement N. 654028) is also gratefully acknowledged for the access in the *In-situ characterization lab in Stiftelsen SINTEF* (Oslo, Norway).

Dr Aitor Arregi acknowledges the University of the Basque Country UPV/EHU for his grant (MOV15/06).

References

[1] S. Manabe, R.T. Wetherald, On the Distribution of Climate Change Resulting from an Increase in CO 2 Content of the Atmosphere, J. Atmos. Sci. 37 (1980) 99–118.

[2] A.A. Olajire, CO_2 capture and separation technologies for end-of-pipe applications-A review, Energy. 35 (2010) 2610–2628. doi:10.1016/j.

[3] L. Fan, Chemical Looping Systems for Fossil Energy, 2010.

[4] International Energy Agency, Energy and Climate Change, 2015. doi:10.1038/479267b.

[5] S. Pacala, R. Socolow, Stabilization Wedges: Solving the Climate Problem for the Next 50 Years with Current Technologies., Science. 305 (2004) 968–972.

[6] H. Yang, Z. Xu, M. Fan, R. Gupta, R.B. Slimane, A.E. Bland, et al., Progress in carbon dioxide separation and capture: A review, J. Environ. Sci. 20 (2008) 14–27.

[7] A.M. Kierzkowska, L.V. Poulikakos, M. Broda, C.R. Müller, Synthesis of calcium-based, Al_2O_3-stabilized sorbents for CO_2 capture using a co-precipitation technique, Int. J. Greenh. Gas Control. 15 (2013) 48–54.

[8] B.P. Mandal, S.S. Bandyopadhyay, Absorption of carbon dioxide into aqueous blends of 2-amino-2-methyl-1-propanol and monoethanolamine, Chem. Eng. Sci. 61 (2006) 5440–5447.

[9] J. Wang, L. Huang, R. Yang, Z. Zhang, J. Wu, Y. Gao, et al., Recent advances in solid sorbents for CO_2 capture and new development trends, Energy Environ. Sci. 7 (2014) 3478–3518.

[10] A.B. Rao, E.S. Rubin, A Technical, Economic, and Environmental Assessment of Amine-Based CO_2 Capture Technology for Power Plant Greenhouse Gas Control, Environ. Sci. Technol. 36 (2002) 4467–4475.

[11] S. Choi, J.H. Drese, C.W. Jones, Adsorbent materials for carbon dioxide capture from large anthropogenic point sources, ChemSusChem. 2 (2009) 796–854.

[12] N. MacDowell, N. Florin, A. Buchard, J. Hallett, A. Galindo, G. Jackson, et al., An overview of CO_2 capture technologies, Energy Environ. Sci. 3 (2010) 1645–1669.

[13] M.S. Yancheshmeh, H.R. Radfarnia, M.C. Iliuta, High temperature CO_2 sorbents and their application for hydrogen production by sorption enhanced steam reforming process, Chem. Eng. J. 283 (2016) 420–444.

[14] C.S. Martavaltzi, A.A. Lemonidou, Development of new CaO based sorbent materials for CO_2 removal at high temperature, Microporous Mesoporous Mater. 110 (2008) 119–127.

[15] C.S. Martavaltzi, T.D. Pefkos, A.A. Lemonidou, Operational window of sorption enhanced steam reforming of methane over CaO-$Ca_{12}Al_{14}O_{33}$, Ind. Eng. Chem.

Res. 50 (2011) 539–545.

[16] J.C. Abanades, D. Alvarez, Conversion Limits in the Reaction of CO_2 with lime, Energy & Fuels. 17 (2003) 308–315.

[17] E.J. Anthony, Ca looping thechnology: current status, developments and future directions, Greenh. Gas Sci. Technol. 1 (2011) 36–47.

[18] H. Gupta, L. Fan, Carbonation - Calcination Cycle Using High Reactivity Calcium Oxide for Carbon Dioxide Separation from Flue Gas, Ind. Eng. Chem. Res. 41 (2002) 4035–4042.

[19] J.M. Valverde, Ca-based synthetic materials with enhanced CO_2 capture efficiency, J. Mater. Chem. A. 1 (2013) 447–468.

[20] N.H. Florin, J. Blamey, P.S. Fennell, Synthetic CaO-Based Sorbent for CO_2 Capture from Large-Point Sources, Energy & Fuels. 24 (2010) 4598–4604.

[21] A. Charitos, C. Hawthorne, A.R. Bidwe, S. Sivalingam, A. Schuster, H. Spliethoff, et al., Parametric investigation of the calcium looping process for CO_2 capture in a 10 kWth dual fluidized bed, Int. J. Greenh. Gas Control. 4 (2010) 776–784.

[22] H. Chen, C. Zhao, W. Yu, Calcium-based sorbent doped with attapulgite for CO_2 capture, Appl. Energy. 112 (2013) 67–74.

[23] C.C. Dean, J. Blamey, N.H. Florin, M.J. Al-Jeboori, P.S. Fennell, The calcium looping cycle for CO_2 capture from power generation, cement manufacture and hydrogen production, Chem. Eng. Res. Des. 89 (2011) 836–855.

[24] V. Manovic, E.J. Anthony, Lime-Based Sorbents for High-Temperature CO_2 Capture-A Review of Sorbent Modification Methods, Int. J. Environ. Res. Public Health. 7 (2010) 3129–3140.

[25] A. Charitos, N. Rodríguez, C. Hawthorne, M. Alonso, M. Zieba, B. Arias, et al.,

Experimental Validation of the Calcium Looping CO_2 Capture Process with Two Circulating Fluidized Bed Carbonator Reactors, Ind. Eng. Chem. Res. 50 (2011) 9685–9695.

[26] R.T. Symonds, D.Y. Lu, R.W. Hughes, E.J. Anthony, A. Macchi, CO_2 Capture from Simulated Syngas via Cyclic Carbonation/Calcination for a Naturally Occurring Limestone: Pilot-Plant Testing, Ind. Eng. Chem. Res. 48 (2009) 8431–8440.

[27] L. Jia, R. Hughes, D. Lu, E.J. Anthony, I. Lau, Attrition of calcining limestones in circulating fluidized-bed systems, Ind. Eng. Chem. Res. 46 (2007) 5199–5209.

[28] D.Y. Lu, R.W. Hughes, E.J. Anthony, Ca-based sorbent looping combustion for CO_2 capture in pilot-scale dual fluidized beds, Fuel Process. Technol. 89 (2008) 1386–1395.

[29] D.C. Ozcan, B.H. Shanks, T.D. Wheelock, Improving the stability of a CaO-based sorbent for CO_2 by thermal pretreatment, Ind. Eng. Chem. Res. 50 (2011) 6933–6942.

[30] V. Manovic, E.J. Anthony, Thermal Activation of CaO-Based Sorbent and Self-Reactivation during CO_2 Capture Looping Cycles, Environ. Sci. Technol. 42 (2008) 4170–4174.

[31] Y. Jie Li, C. Sui Zhao, L. Bo Duan, C. Liang, Q. Zhao Li, W. Zhou, et al., Cyclic calcination/carbonation looping of dolomite modified with acetic acid for CO_2 capture, Fuel Process. Technol. 89 (2008) 1461–1469.

[32] H. Chen, C. Zhao, M. Chen, Y. Li, X. Chen, CO_2 uptake of modified calcium-based sorbents in a pressurized carbonation-calcination looping, Fuel Process. Technol. 92 (2011) 1144–1151.

[33] B. Arias, G.S. Grasa, J.C. Abanades, Effect of sorbent hydration on the average

activity of CaO in a Ca-looping system, Chem. Eng. J. 163 (2010) 324–330.

[34] J. Yin, C. Zhang, C. Qin, W. Liu, H. An, G. Chen, et al., Reactivation of calcium-based sorbent by water hydration for CO_2 capture, Chem. Eng. J. 198–199 (2012) 38–44.

[35] F. Zeman, Effect of steam hydration on performance of lime sorbent for CO_2 capture, Int. J. Greenh. Gas Control. 2 (2008) 203–209.

[36] S.D. Angeli, C.S. Martavaltzi, A.A. Lemonidou, Development of a novel-synthesized Ca-based CO_2 sorbent for multicycle operation: Parametric study of sorption, Fuel. 127 (2014) 62–69.

[37] M. Broda, C.R. Müller, Sol-gel-derived, CaO-based, ZrO_2-stabilized CO_2 sorbents, Fuel. 127 (2014) 94–100.

[38] R. Koirala, K.R. Gunugunuri, S.E. Pratsinis, P.G. Smirniotis, Effect of zirconia doping on the structure and stability of CaO-based sorbents for CO_2 capture during extended operating cycles, J. Phys. Chem. C. 115 (2011) 24804–24812.

[39] H. Lu, E.P. Reddy, P.G. Smirniotis, Calcium oxide based sorbents for capture of carbon dioxide at high temperatures, Ind. Eng. Chem. Res. 45 (2006) 3944–3949.

[40] J. Park, K.B. Yi, Effects of preparation method on cyclic stability and CO_2 absorption capacity of synthetic CaO-MgO absorbent for sorption-enhanced hydrogen production, Int. J. Hydrogen Energy. 37 (2012) 95–102.

[41] C. Zhao, Z. Zhou, Z. Cheng, Sol–gel-Derived Synthetic CaO-Based CO_2 Sorbents Incorporated with Different Inert Materials, Ind. Eng. Chem. Res. 53 (2014) 14065–14074.

[42] H.R. Radfarnia, M.C. Iliuta, Metal oxide-stabilized calcium oxide CO_2 sorbent for multicycle operation, Chem. Eng. J. 232 (2013) 280–289.

[43] Z. Zhou, Y. Qi, M. Xie, Z. Cheng, W. Yuan, Synthesis of CaO-based sorbents

through incorporation of alumina/aluminate and their CO_2 capture performance, Chem. Eng. Sci. 74 (2012) 172–180.

[44] G.K. Reddy, S. Quillin, P. Smirniotis, Influence of the Synthesis Method on the Structure and CO_2 Adsorption Properties of Ca/Zr Sorbents, Energy & Fuels. 28 (2014) 3292–3299.

[45] Z. Li, N. Cai, Y. Huang, H. Han, Synthesis, Experimental Studies, and Analysis of a New Calcium-Based Carbon Dioxide Adsorbent, Energy & Fuels. 19 (2005) 1447–1452.

[46] M. Broda, C.R. Müller, Synthesis of highly efficient, Ca-based, Al_2O_3-stabilized, carbon gel-templated CO_2 sorbents., Adv. Mater. 24 (2012) 3059–3064.

[47] C. Luo, Y. Zheng, C. Zheng, J. Yin, C. Qin, B. Feng, Manufacture of calcium-based sorbents for high temperature cyclic CO_2 capture via a sol-gel process, Int. J. Greenh. Gas Control. 12 (2013) 193–199.

[48] A. Antzara, E. Heracleous, A.A. Lemonidou, Improving the stability of synthetic CaO-based CO_2 sorbents by structural promoters, Appl. Energy. 156 (2015) 331–343.

[49] A. Antzara, E. Heracleous, A.A. Lemonidou, Energy efficient sorption enhanced-chemical looping methane reforming process for high-purity H_2 production: Experimental proof-of-concept, Appl. Energy. 180 (2016) 457–471.

[50] Z. Skoufa, A. Antzara, E. Heracleous, A.A. Lemonidou, Evaluating the Activity and Stability of CaO-based Sorbents for Post-combustion CO_2 Capture in Fixed-bed Reactor Experiments, Energy Procedia. 86 (2016) 171–180.

[51] S. Yang, Y. Xiao, Steam Catalysis in CaO Carbonation under Low Steam Partial Pressure, Ind. Eng. Chem. Res. 47 (2008) 4043–4048.

[52] M. Zhang, Y. Peng, Y. Sun, P. Li, J. Yu, Preparation of CaO-Al_2O_3 sorbent and

CO_2 capture performance at high temperature, Fuel. 111 (2013) 636–642.

[53] H.R. Radfarnia, A. Sayari, A highly efficient CaO-based CO_2 sorbent prepared by a citrate-assisted sol–gel technique, Chem. Eng. J. 262 (2015) 913–920.

[54] N.J. Amos, M. Widyawati, S. Kureti, D. Trimis, A.I. Minett, A.T. Harris, et al., Design and synthesis of stable supported-CaO sorbents for CO_2 capture, J. Mater. Chem. A. 2 (2014) 4332–4339.

[55] M. Broda, V. Manovic, E.J. Anthony, C.R. Müller, Effect of pelletization and addition of steam on the cyclic performance of carbon-templated, CaO-based CO_2 sorbents, Environ. Sci. Technol. 48 (2014) 5322–5328.

[56] G.S. Grasa, J.C. Abanades, CO_2 Capture Capacity of CaO in Long Series of Carbonation/Calcination Cycles, Ind. Eng. Chem. Res. 45 (2006) 8846–8851.

[57] F.N. Ridha, V. Manovic, Y. Wu, A. Macchi, E.J. Anthony, Pelletized CaO-based sorbents treated with organic acids for enhanced CO_2 capture in Ca-looping cycles, Int. J. Greenh. Gas Control. 17 (2013) 357–365.

[58] S. Ergun, Fluid flow through packed columns, Chem. Eng. Prog. 48 (1952) 89–94.

[59] C.Y. Wen, Y.H. Yu, Mechanics of fluidization, Chem. Eng. Prog. Symp. Ser. 62 (1966) 100–111.

[60] J.G. Yates, Some fundamental aspects of fluidization, in: Fundam. Fluid. Chem. Process., 1983: p. 230.

[61] L.S. Ferreira, J.O. Trierweiler, Modeling and simulation of the polymeric nanocapsule formation process, IFAC Proc. 7 (2009) 405–410.

[62] R. Barker, The reversibility of the reaction $CaCO_3 \rightleftarrows CaO+CO_2$, J. Appl. Chem. Biotechnol. 23 (1973) 733–742.

[63] L-S. Fan, L. Zeng, W. Wang, S. Luo, Chemical looping processes for CO_2

capture and carbonaceous fuel conversion – prospect and opportunity, Energy Environ. Sci. 5 (2012) 7254.

[64] Y. Wang, W.J. Thomson, The Effects of Steam and Carbon-Dioxide on Calcite Decomposition Using Dynamic X-Ray-Diffraction, Chem. Eng. Sci. 50 (1995) 1373–1382.

[65] F-C. Yu, N. Phalak, Z. Sun, L-S. Fan, Activation Strategies for Calcium-Based Sorbents for CO_2 Capture: A Perspective, Ind. Eng. Chem. Res. 51 (2012) 2133–2142.

[66] F. Donat, N.H. Florin, E.J. Anthony, P.S. Fennell, Influence of high-temperature steam on the reactivity of CaO sorbent for CO_2 capture, Environ. Sci. Technol. 46 (2012) 1262–1269.

[67] V. Manovic, E.J. Anthony, Carbonation of CaO-based sorbents enhanced by steam addition, Ind. Eng. Chem. Res. 49 (2010) 9105–9110.

[68] A.A. Mitchell, Flue Gas Analysis, in: Gas Appl. Eng. Handb., 2006.

[69] R.T. Symonds, D.Y. Lu, V. Manovic, E.J. Anthony, Pilot-Scale Study of CO_2 Capture by CaO-Based Sorbents in the Presence of Steam and SO_2, Ind. Eng. Chem. Res. 51 (2012) 7177–7184.

[70] D. Alvarez, J.C. Abanades, Determination of the Critical Product Layer Thickness in the Reaction of CaO with CO_2, Ind. Eng. Chem. Res. 44 (2005) 5608–5615.

[71] J. Blamey, M.J. Al-Jeboori, V. Manovic, P.S. Fennell, E.J. Anthony, CO_2 capture by calcium aluminate pellets in a small fluidized bed, Fuel Process. Technol. 142 (2016) 100–106.

[72] V. Manovic, J.P. Charland, J. Blamey, P.S. Fennell, D.Y. Lu, E.J. Anthony, Influence of calcination conditions on carrying capacity of CaO-based sorbent in

CO_2 looping cycles, Fuel. 88 (2009) 1893–1900.

[73] D.Y. Lu, R.W. Hughes, E.J. Anthony, V. Manovic, Sintering and Reactivity of $CaCO_3$-Based Sorbents for In Situ CO_2 Capture in Fluidized Beds under Realistic Calcination Conditions, J. Environ. Eng. 135 (2009) 404–410.

[74] Z. Jiang, L. Duan, X. Chen, C. Zhao, Effect of Water Vapor on Indirect Sulfation during Oxy-fuel Combustion, Energy & Fuels. 27 (2013) 1506–1512.

[75] H. Lu, P.G. Smirniotis, Calcium Oxide Doped Sorbents for CO_2 Uptake in the Presence of SO_2 at High Temperatures, Ind. Eng. Chem. Res. 48 (2009) 5454–5459.

[76] C. Luo, Y. Zheng, J. Yin, C. Qin, N. Ding, C. Zheng, et al., Effect of Support Material on Carbonation and Sulfation of Synthetic CaO-based Sorbents in Calcium Looping Cycle, Energy & Fuels. 27 (2013) 4824–4831.

[77] Z. Yang, M. Zhao, N.H. Florin, A.T. Harris, Synthesis and Characterization of CaO Nanopods for High Temperature CO_2 Capture, Ind. Eng. Chem. Res. 48 (2009) 10765–10770.

[78] X-C. Chen, J-P. Zhou, H.-Y. Wang, P.-S. Xu, G.-Q. Pan, *In situ* high temperature X-ray diffraction studies of ZnO thin film, Chinese Phys. B. 20 (2011) 96102.

[79] I. Martinez, G. Grasa, R. Murillo, B. Arias, J.C. Abanades, Evaluation of CO_2 Carrying Capacity of Reactivated CaO by Hydration, Energy Fuels. 25 (2011) 1294–1301.

[80] Y. Álvarez Criado, M. Alonso, J.C. Abanades, Composite Material for Thermochemical Energy Storage Using $CaO/Ca(OH)_2$, Ind. Eng. Chem. Res. 54 (2015) 9314–9327.

[81] V. Manovic, D. Lu, E.J. Anthony, Steam hydration of sorbents from a dual fluidized bed CO_2 looping cycle reactor, Fuel. 87 (2008) 3344–3352.

[82] I. Fujii, M. Ishino, S. Akiyama, M.S. Murthy, K.S. Rajanandam, Behavior of $Ca(OH)_2$/CaO pellet under dehydration and hydration, Sol. Energy. 53 (1994) 329–341.

[83] F. Scala, A. Cammarota, R. Chirone, P. Salatino, I. Chimica, U. Federico, Comminution of Limestone During Batch Fluidized-Bed Calcination and Sulfation, AIChE J. 43 (1997) 363–373.

[84] F. Scala, P. Salatino, R. Boerefijn, M. Ghadiri, Attrition of sorbents during fluidized bed calcination and sulphation, Powder Technol. 107 (2000) 153–167.

[85] D. Kunii, O. Levenspiel, Fluidization and Mapping of Regimes, in: Fluid. Eng., Elsevier, 1991: pp. 61–94.

[86] J. Pata, M. Hartman, Minimum Fluidization Velocities of Lime and Limestone Particles, Ind. Eng. Chem. Process Des. Dev. 17 (1978) 231–236.

Figure Captions:

Figure 1: Effect of pelletization in the performance of the $CaO/CaZrO_3$ sorbent during multiple carbonation/calcination cycles in TGA (*Carbonation:* 650°C, 15% CO_2/N_2, 30 min, *Calcination:* 850°C, 100% N_2, 5 min)

Figure 2: CaO conversion and sorption capacity during pre-breakthrough period for (a) cycles 1-15 and (b) cycles 16-26 after extended carbonation in cycle 16, for the $CaO/CaZrO_3$ sorbent in fluidized bed experiments with different fluidization velocities (*carbonation:* 650ºC, 10% CO_2/3.2% O_2/N_2, GHSV=3500 h^{-1}; *calcination:* 800ºC, 100%/N_2, GHSV=3100 h^{-1}). Note: Open symbols in cycles 1 and 16 refer to overall conversion.

Figure 3: Percentage of CO_2 captured by the $CaO/CaZrO_3$ sorbent with different fluidization velocities during carbonation stage of 1st **(a)** and 16th cycle **(b)** (*carbonation:* 650ºC, 10% CO_2/3.2% O_2/N_2, GHSV=3500 h^{-1}; *calcination:* 800ºC, 100% N_2; GHSV=3100 h^{-1}).

Figure 4: CaO conversion and sorption capacity **(a)** and CO_2 capture **(b)** during pre-breakthrough period versus number of cycle for $CaO/CaZrO_3$ sorbent in fluidized bed experiments with different space velocities (*carbonation:* 650ºC, 10% CO_2/3.2% O_2/N_2; *calcination:* 800ºC, 100% N_2; U/U_{mf}=2.5).

Figure 5: Effect of steam in CaO conversion and sorption capacity during pre-breakthrough period versus number of cycles for $CaO/CaZrO_3$ sorbent (dry conditions: *carbonation: 650ºC, 10% CO_2/3.2% O_2/N_2,* GHSV=2000 h^{-1}*; calcination: 800ºC, 100%/N_2, GHSV= 1700 h^{-1}; U/U_{mf} =2.5* | wet conditions: *carbonation: 650ºC, 10% CO_2/3.2% O_2/20% H_2O/N_2,* GHSV=2500 h^{-1}*; calcination: 800ºC, 20% H_2O/N_2, GHSV= 2150 h^{-1}; U/U_{mf}= 3.1*).

Figure 6: Pore size distribution of the fresh and used $CaO/CaZrO_3$ CO_2 sorbent under dry and wet conditions

Figure 7: Effect of steam on the percentage of CO_2 captured by the sorbent during 1st **(a)** and 20th cycle **(b)** (dry conditions: *carbonation: 650ºC, 10% CO_2/3.2% O_2/N_2,* GHSV=2000 h^{-1}*; calcination: 800ºC, 100%/N_2, GHSV= 1700 h^{-1}; U/U_{mf} =2.5* | wet conditions: *carbonation: 650ºC, 10% CO_2/3.2% O_2/20% H_2O/N_2,* GHSV=2500 h^{-1}*; calcination: 800ºC, 20% H_2O/N_2, GHSV= 2150 h^{-1}; U/U_{mf} = 3.1*).

Figure 8: CO_2 sorption capacity and CaO conversion during pre-breakthrough period versus number of cycles for $CaO/CaZrO_3$ sorbent in fluidized bed experiments at different carbonation and calcination temperatures (*carbonation:* 10% CO_2/3.2% O_2/20% H_2O/N_2, GHSV= 2500 h^{-1}; *calcination:* 20%H_2O/N_2, GHSV= 2150 h^{-1}; U/U_{mf} =3.1).

Figure 9: Percentage of CO_2 captured during carbonation stage of 1st and 20th cycle at different temperature protocols: **(a)** H-ΔT test and **(b)** L-ΔT test (*carbonation:* 10% CO_2/3.2% O_2/20% H_2O/N_2, GHSV= 2500 h^{-1}; *calcination:* 20%H_2O/N_2, GHSV= 2150 h^{-1}; U/U_{mf}=3.1).

Figure 10: CO_2 sorption capacity and CaO conversion during pre-breakthrough period versus number of cycles for calcined limestone **(a)** and $CaO/CaZrO_3$ sorbent **(b)** in fluidized bed experiments under severe calcination conditions (*carbonation:* 650ºC, 10% CO_2/3.2% O_2/20% H_2O/N_2, $GHSV_{limestone}$=3650 h^{-1}, $GHSV_{CaO/CaZrO3}$=2500 h^{-1}; *calcination:* 920ºC, 20%H_2O/CO_2, $GHSV_{limestone}$=2850 h^{-1}, $GHSV_{CaO/CaZrO3}$=2150 h^{-1}; U/U_{mf}=3.1).

Figure 11: Percentage of CO_2 captured during carbonation stage of 1st and 20th cycle for calcined limestone **(a)** and $CaO/CaZrO_3$ sorbent **(b)** in fluidized bed experiments

under severe calcination conditions (*carbonation:* 650ºC, 10% CO_2/3.2% O_2/20% H_2O/N_2, $GHSV_{limestone}$=3650 h^{-1}, $GHSV_{CaO/CaZrO3}$=2500 h^{-1}; *calcination:* 920ºC, 20%H_2O/CO_2, $GHSV_{limestone}$=2850 h^{-1}, $GHSV_{CaO/CaZrO3}$=2150 h^{-1}; U/U_{mf}=3.1).

Figure 12: SEM images of the fresh $CaO/CaZrO_3$ CO_2 sorbent material **(a & b)** and the spent material after cyclic carbonation/calcination experiments in the absence of steam (**c & d**) and in the presence of steam at different carbonation and calcination temperatures (**e & f:** *carbonation at 650°C; calcination at 800°C,* **g & h:** *carbonation at 680°C; calcination at 750°C*)

Figure 13: Main peaks of $CaCO_3$ and CaO in the XRD diffractograms of the used materials: **(a)** carbonation at 650°C and calcination at 800°C, **(b)** carbonation at 680°C and calcination at 750°C

Figure 14: CaO conversion of fresh and used $CaO/CaZrO_3$ CO_2 sorbent during the in-situ XRD and fluidized bed carbonation/calcination experiments: **(a)** carbonation at 650°C and calcination at 800°C, **(b)** carbonation at 680°C and calcination at 750°C

Figure 15: Particle size distribution of: **(a)** $CaO/CaZrO_3$ CO_2 sorbent before and after different experimental protocols under mild calcination conditions and **(b)** $CaO/CaZrO_3$ CO_2 sorbent and calcined limestone before and after carbonate looping cycles under severe calcination conditions (T=920°C, 20 vol.%H_2O/CO_2).

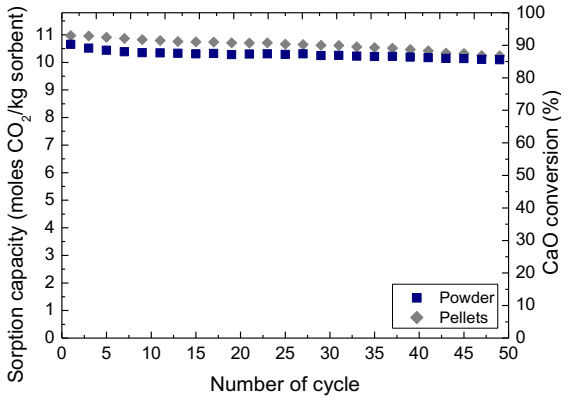
Sorption capacity (moles CO2/kg sorbent)
CaO conversion (%)
Number of cycle
Powder
Pellets
0
1
2
3
4
5
6
7
8
9
10
11
0
10
20
30
40
50
60
70
80
90
100
0
5
10
15
20
25
30
35
40
45
50

Figure 1

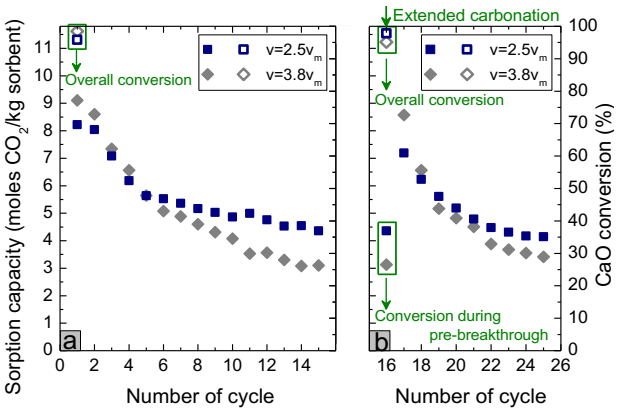
Sorption capacity (moles CO2/kg sorbent)
Overall conversion
v=2.5vm
v=3.8vm
a
Number of cycle
Extended carbonation
Overall conversion
Conversion during
pre-breakthrough
b
Number of cycle
CaO conversion (%)

Figure 2

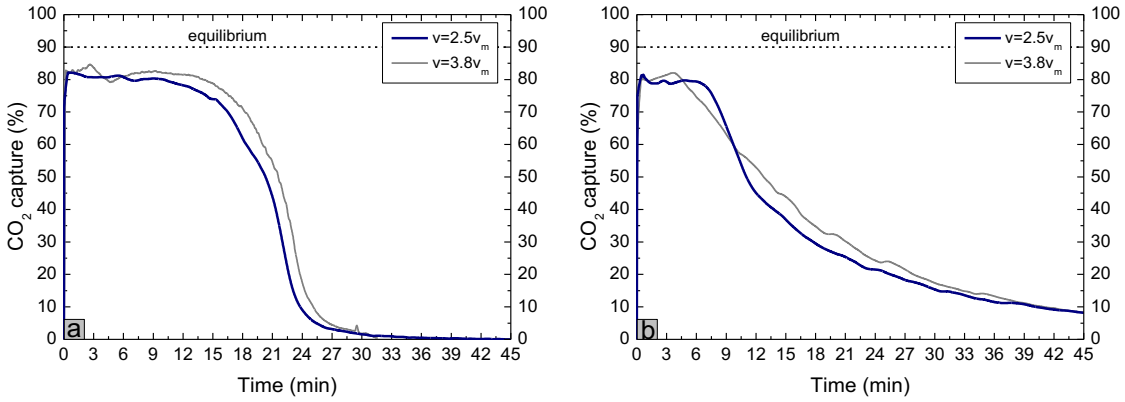

Figure 3

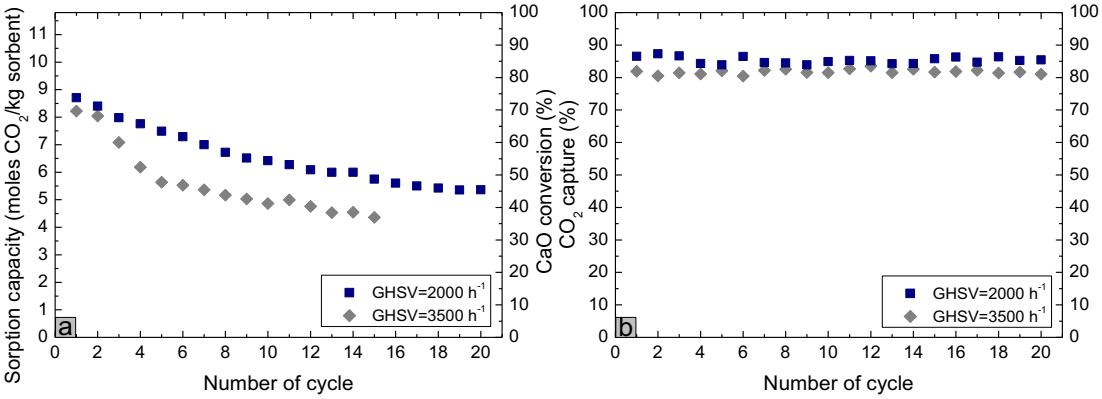
Sorption capacity (moles CO2/kg sorbent)
CaO conversion (%)
CO2 capture (%)
Number of cycle
Number of cycle
GHSV=2000 h-1
GHSV=3500 h-1
GHSV=2000 h-1
GHSV=3500 h-1
a
b

Figure 4

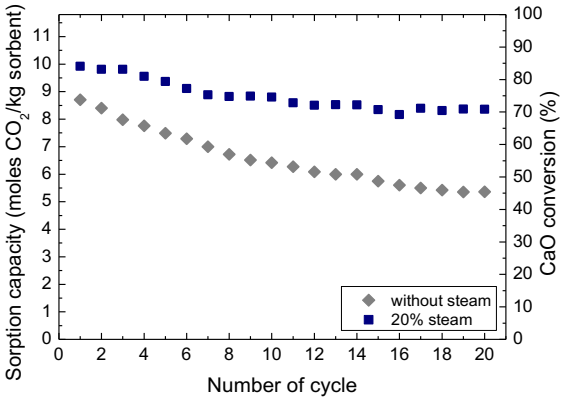
Sorption capacity (moles CO2/kg sorbent)
CaO conversion (%)
Number of cycle
without steam
20% steam
0
1
2
3
4
5
6
7
8
9
10
11
0
10
20
30
40
50
60
70
80
90
100
0
2
4
6
8
10
12
14
16
18
20

Figure 5

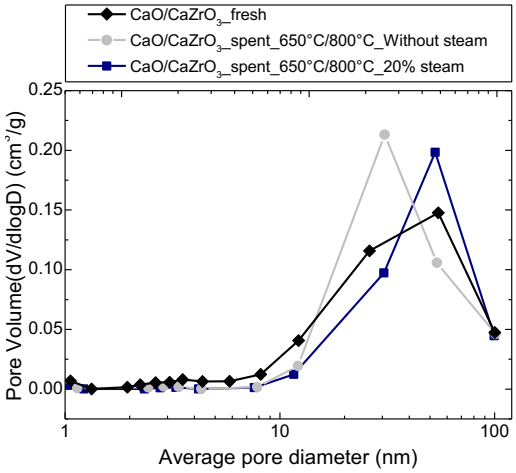
CaO/CaZrO3_fresh
CaO/CaZrO3_spent_650°C/800°C_Without steam
CaO/CaZrO3_spent_650°C/800°C_20% steam
Pore Volume(dV/dlogD) (cm³/g)
0.25
0.20
0.15
0.10
0.05
0.00
1
10
100
Average pore diameter (nm)

Figure 6

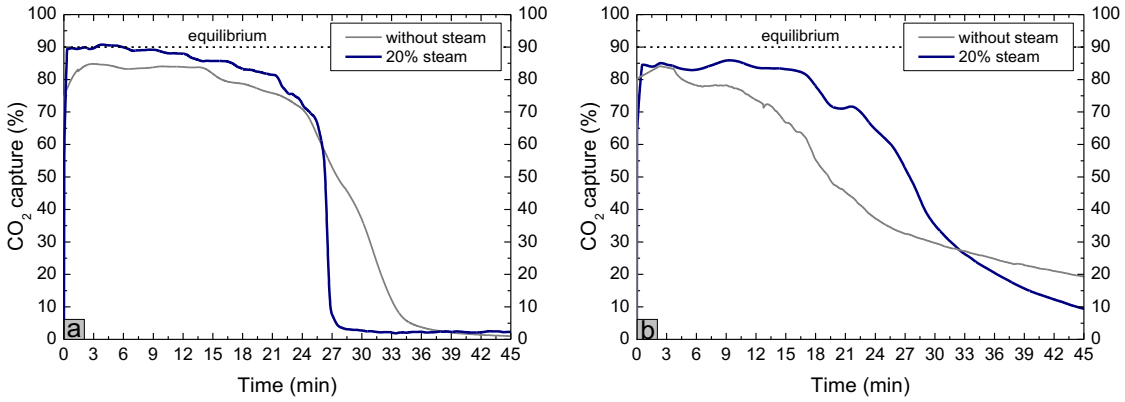

Figure 7

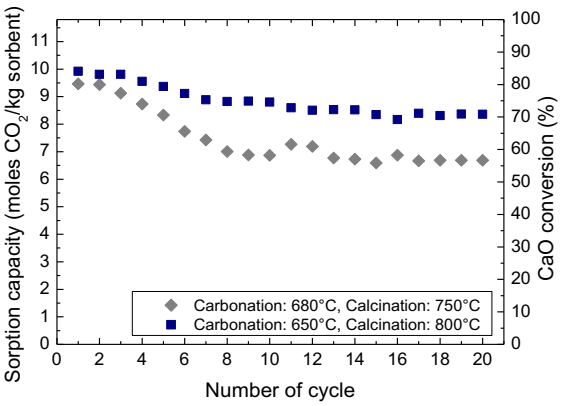
Sorption capacity (moles CO2/kg sorbent)
CaO conversion (%)
Number of cycle
Carbonation: 680°C, Calcination: 750°C
Carbonation: 650°C, Calcination: 800°C

Figure 8

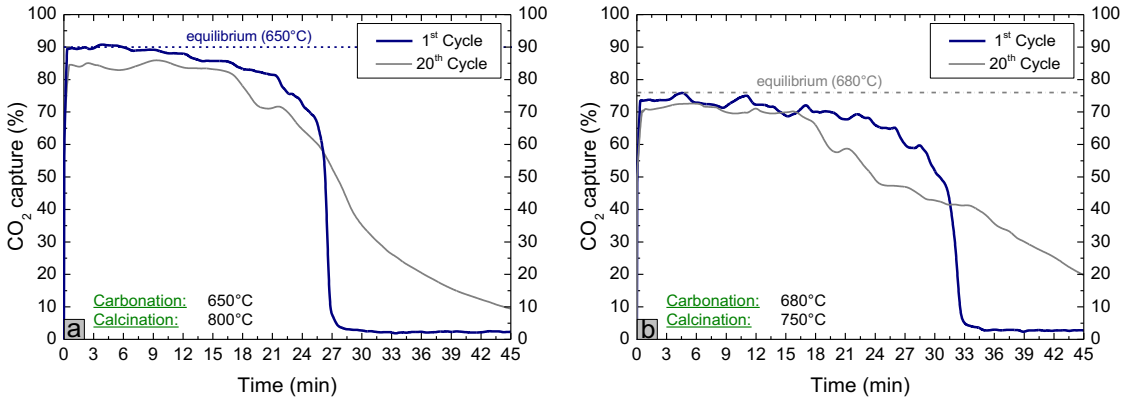
equilibrium (650°C)
1st Cycle
20th Cycle
CO2 capture (%)
Carbonation: 650°C
Calcination: 800°C
a
Time (min)
equilibrium (680°C)
1st Cycle
20th Cycle
CO2 capture (%)
Carbonation: 680°C
Calcination: 750°C
b
Time (min)

Figure 9

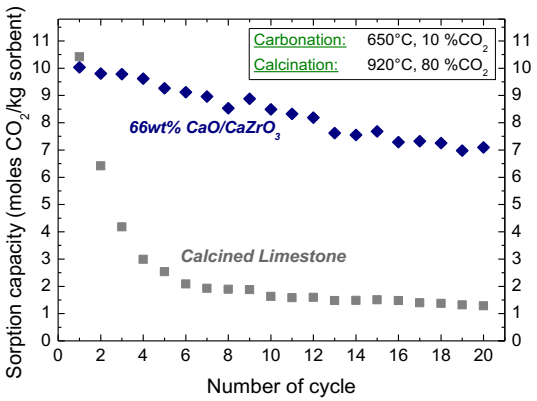
Carbonation: 650°C, 10 %CO2
Calcination: 920°C, 80 %CO2
66wt% CaO/CaZrO3
Calcined Limestone
Sorption capacity (moles CO2/kg sorbent)
Number of cycle
0
1
2
3
4
5
6
7
8
9
10
11
0
2
4
6
8
10
12
14
16
18
20

Figure 10

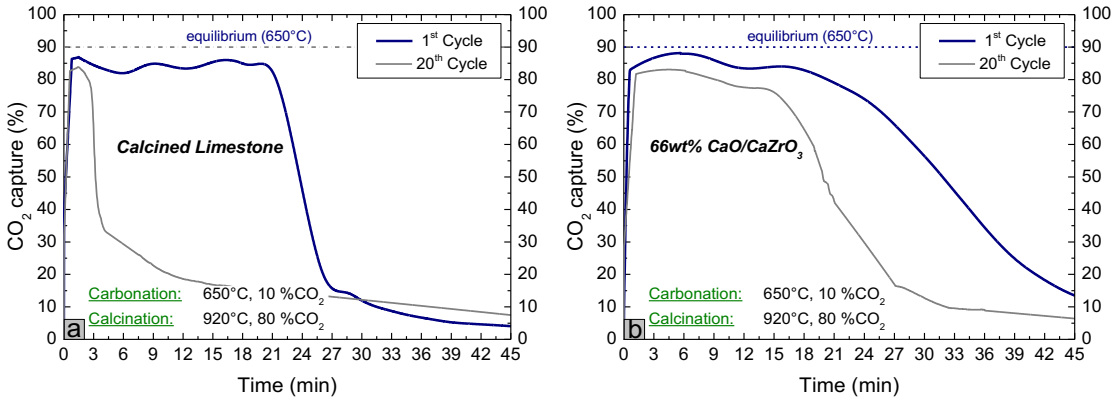
equilibrium (650°C)
1st Cycle
20th Cycle
Calcined Limestone
Carbonation: 650°C, 10 %CO2
Calcination: 920°C, 80 %CO2
a
CO2 capture (%)
Time (min)
equilibrium (650°C)
1st Cycle
20th Cycle
66wt% CaO/CaZrO3
Carbonation: 650°C, 10 %CO2
Calcination: 920°C, 80 %CO2
b
CO2 capture (%)
Time (min)

Figure 11

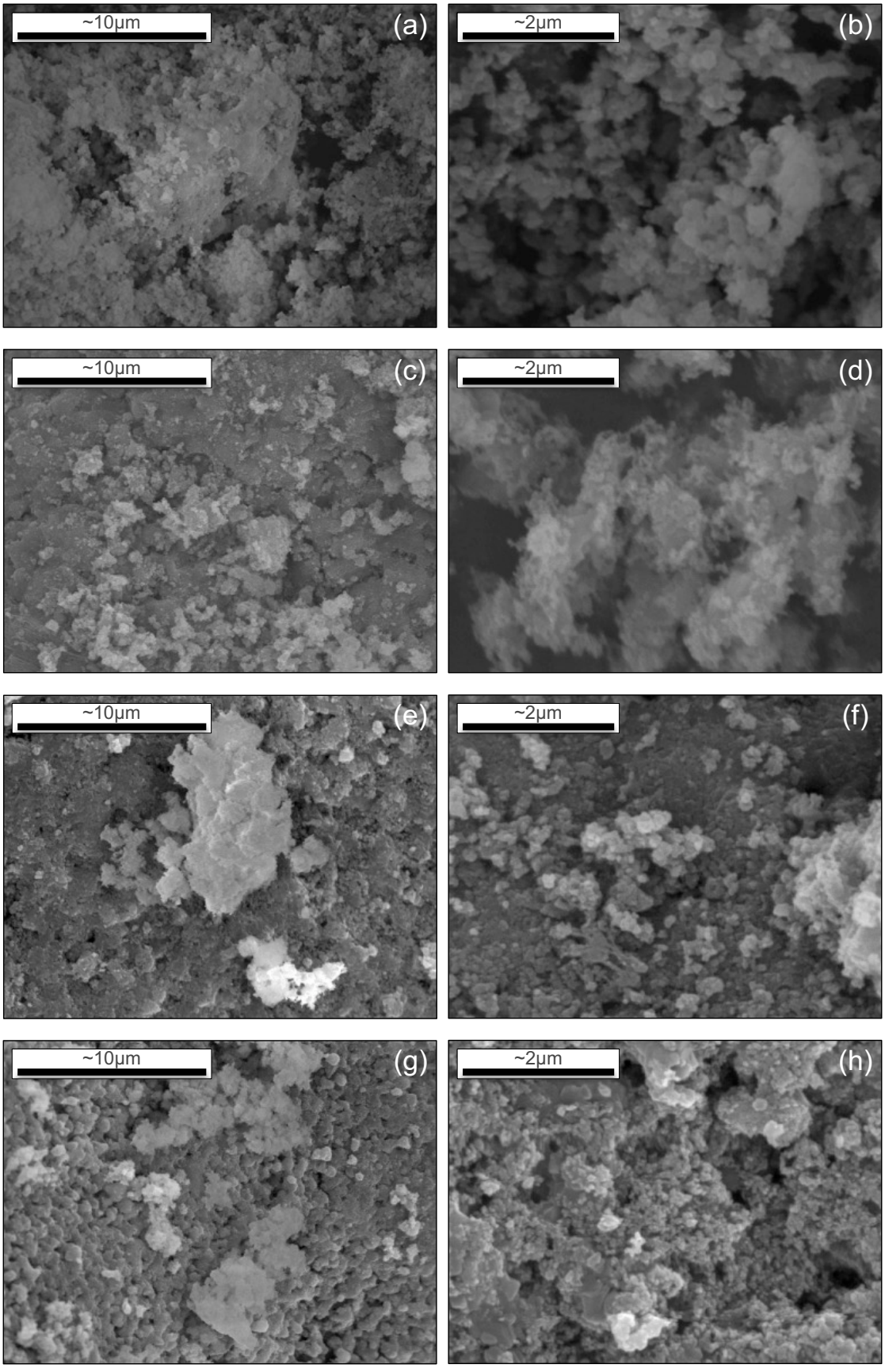

Figure 12

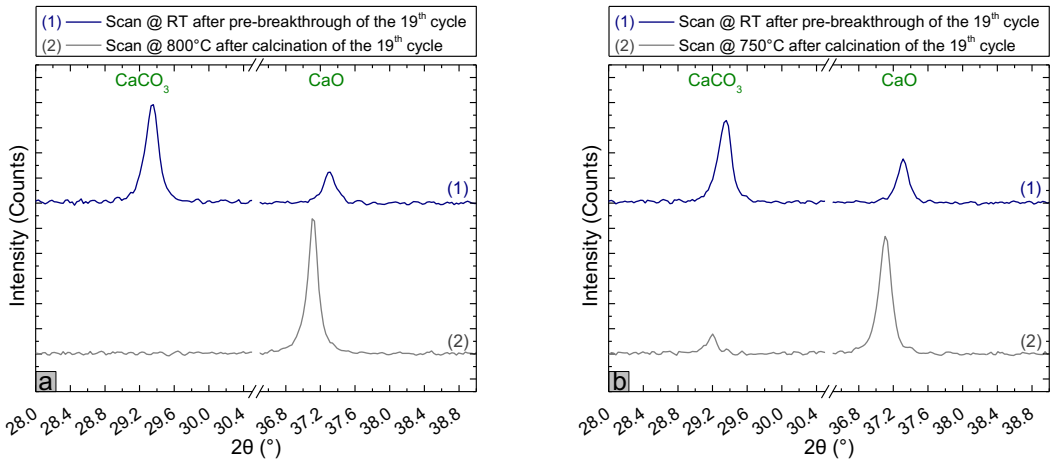
(1) Scan @ RT after pre-breakthrough of the 19th cycle
(2) Scan @ 800°C after calcination of the 19th cycle
CaCO3
CaO
Intensity (Counts)
(1)
(2)
a
28.0 28.4 28.8 29.2 29.6 30.0 30.4 36.8 37.2 37.6 38.0 38.4 38.8
2θ (°)
(1) Scan @ RT after pre-breakthrough of the 19th cycle
(2) Scan @ 750°C after calcination of the 19th cycle
CaCO3
CaO
Intensity (Counts)
(1)
(2)
b
28.0 28.4 28.8 29.2 29.6 30.0 30.4 36.8 37.2 37.6 38.0 38.4 38.8
2θ (°)

Figure 13

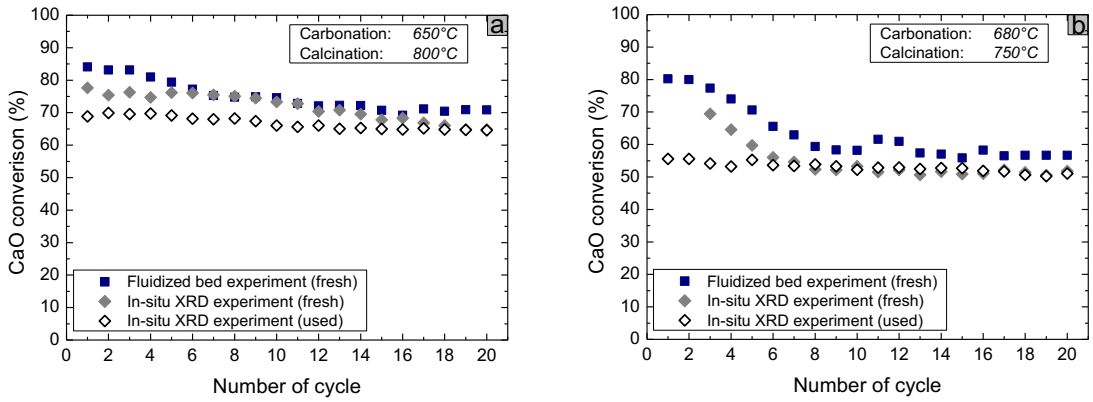
a
Carbonation: 650°C
Calcination: 800°C
Fluidized bed experiment (fresh)
In-situ XRD experiment (fresh)
In-situ XRD experiment (used)
CaO converison (%)
Number of cycle
b
Carbonation: 680°C
Calcination: 750°C
Fluidized bed experiment (fresh)
In-situ XRD experiment (fresh)
In-situ XRD experiment (used)
CaO converison (%)
Number of cycle

Figure 14

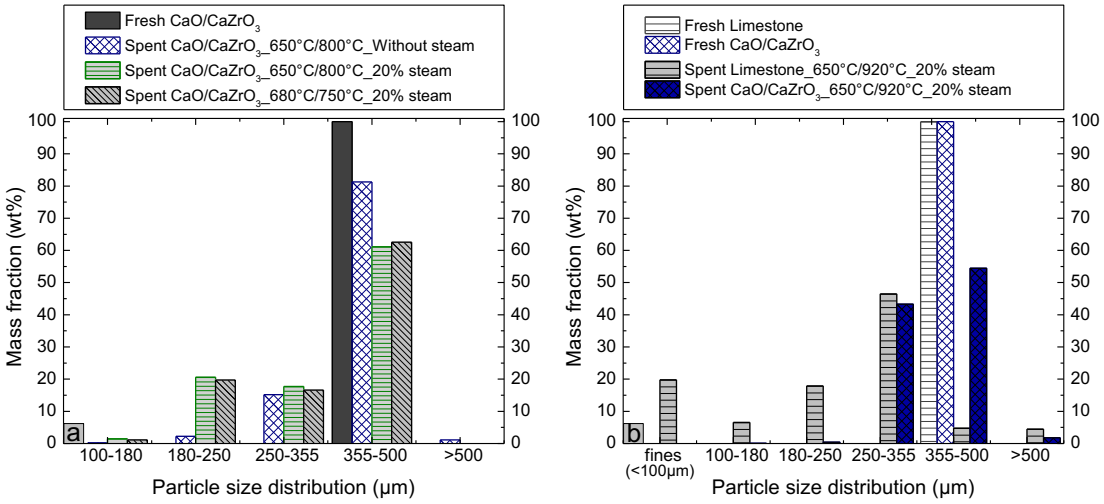
Fresh CaO/CaZrO3
Spent CaO/CaZrO3_650°C/800°C_Without steam
Spent CaO/CaZrO3_650°C/800°C_20% steam
Spent CaO/CaZrO3_680°C/750°C_20% steam
Mass fraction (wt%)
Particle size distribution (μm)
100-180
180-250
250-355
355-500
>500
a
Fresh Limestone
Fresh CaO/CaZrO3
Spent Limestone_650°C/920°C_20% steam
Spent CaO/CaZrO3_650°C/920°C_20% steam
fines
(<100μm)
b

Figure 15